Kriging Surrogate Model-Based Design of an Ultra-High-Speed Surface-Mounted Permanent-Magnet Synchronous Motor Considering Stator Iron Loss and Rotor Eddy Current Loss

So-Yeon Im[1], Soo-Gyung Lee[2], Dong-Min Kim[3], Gu Xu[1], Sun-Yong Shin[1], and Myung-Seop Lim[1]

[1]Department of Automotive Engineering (Automotive-Computer Convergence), Hanyang University, Seoul 04763, South Korea

[2]Steel Solution Research and Development Center, POSCO Global Research and Development Center, Incheon 21985, South Korea

[3]Department of Automotive Engineering, Honam University, Gwangju 62399, South Korea

Ultra-high-speed (UHS) surface-mounted permanent-magnet synchronous motors (SPMSMs) are widely used for driving air compressors. UHS SPMSMs can suffer from high stator iron loss and rotor eddy current loss due to their high rotational speed and changes in the magnetic flux density when loading. Since these losses do not have a linear trend but change according to the motor design parameters, mathematical models cannot always predict them. This study aims to design UHS SPMSMs based on a kriging surrogate model that takes into account the stator iron loss and rotor eddy current loss. Since the kriging surrogate model is highly predictive for nonlinear inputs, it is the perfect candidate to take into account the stator iron loss and rotor eddy current loss. The design proposed in this study allowed to minimize the size and losses of a motor that satisfied the power specification.

Index Terms—**Eddy current loss, kriging surrogate model, stator iron loss, ultra-high-speed (UHS) motor.**

I. Introduction

ULTRA-HIGH-SPEED (UHS) surface-mounted permanent-magnet synchronous motors (SPMSMs) are widely used for driving air compressors that supply high flow and high-pressure oxygen [1], [2]. The electromagnetic losses of a UHS SPMSM include iron loss and copper loss. In particular, a UHS SPMSM can suffer from a high stator iron loss and rotor eddy current loss due to its high rotational speed [3]. In fact, when the motor is magnetized by an alternating current (ac), the hysteresis loss is proportional to the frequency, and the eddy current loss is proportional to the square of the frequency [4]. These losses are related to motor saturation; since the saturation varies according to the density of the magnetic flux, they do not follow a linear trend. Therefore, the nonlinearity of the motor losses must be taken into consideration for the design of the motor. To ensure mechanical stability, UHS SPMSMs are manufactured with a sleeve outside the permanent magnet (PM) [5]. The sleeve is not a magnetic material but has electrical conduction properties such as those of a PM and strongly contributes to the rotor eddy current loss.

In this article, the design of an initial model, obtained through a conventional design methodology, and a kriging surrogate model-based design are described and compared. The kriging surrogate model is suitable for the design of electric motors because it is highly predictive when nonlinear inputs are used [6]. The design of UHS SPMSM has reduced the stator iron loss and rotor eddy current loss using the kriging surrogate model.

Manuscript received March 16, 2021; revised April 30, 2021; accepted May 11, 2021. Date of publication May 13, 2021; date of current version January 20, 2022. Corresponding author: M.-S. Lim (e-mail: myungseop@hanyang.ac.kr).

Color versions of one or more figures in this article are available at https://doi.org/10.1109/TMAG.2021.3080119.

Digital Object Identifier 10.1109/TMAG.2021.3080119

TABLE I
Target Specifications

Parameters	Value	Unit
Pole / Slot	2 / 6	-
Maximum stator diameter	115	mm
Maximum rotor diameter	27	mm
Maximum stack length	75	mm
Maximum rotational speed	110	krpm
Current density	8.5	A_{rms}/mm^2
Slot fill factor	60	%

The contribution of this article is to present a two-step optimal design process that considers the accuracy and computation time through the kriging surrogate model. The presented process is divided into two steps: size determination and loss minimization. This design process reduces the computation time by 20 times compared with when the rotor eddy current loss is considered in the first step.

II. Conventional Model

The specifications of the model are listed in Table I. Here, the maximum stator diameter, the maximum rotor diameter, and the maximum stack length are the values normalized based on the maximum stator diameter. Since the frequency of the input current is high due to the UHS of the motor, the number of poles is set to 2 [4], [5]. The maximum rotational speed is 110 kr/min.

The purpose of the initial design is to increase the output power density (by reducing the stack length reported in the specifications) while maintaining the same output power. To operate the rotor safely, it is essential to design the rotor taking into account the mechanical stress [7], the tolerance of the shrink fit, and the temperature at the maximum rotational speed. The materials used for the rotor are as follows: Sm_2Co_{17}

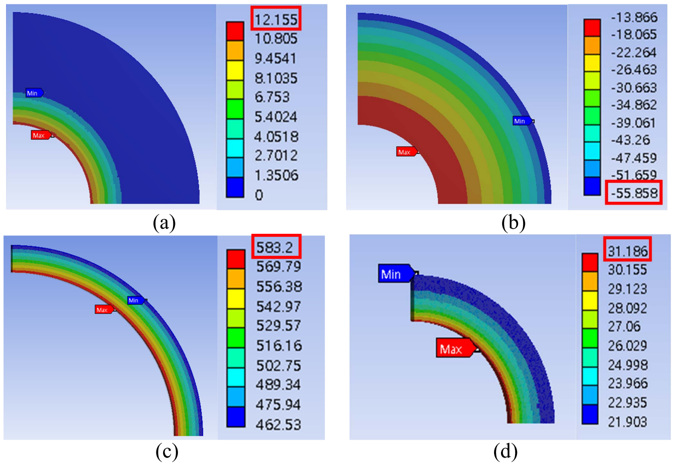

Fig. 1. Stress distribution at 121 kr/min. (a) PM maximum principal stress. (b) PM minimum principal stress. (c) Sleeve von-Mises stress. (d) Shaft von-Mises stress.

TABLE II
ROTOR FEA RESULT FROM ANSYS AT 121 Kr/Min

Items	2D FEA (ANSYS)
Permanent magnet principal stress *a*, *b* (safety factor)	12.16 MPa, -55.86MPa (3.46)
Sleeve Max. von Mises stress (safety factor)	583.20 MPa (1.78)
Shaft Max. von Mises stress (MPa) (safety factor)	31.19 MPa (32.07)

a: Permanent magnet maximum principal stress / *b*: Permanent magnet minimum principal stress

for the PM, Inconel 718 for the sleeve, and SUS630 for the shaft. Fig. 1 and Table II show the mechanical stress with ANSYS, a two-dimensional finite element analysis (2D FEA). The safety factor of the sleeve, when 110% of the maximum rotational speed is used, is 1.78. This value ensures an acceptable mechanical stability in the structure of the rotor [8]. For the reason, the safety factor of the sleeve is set within the range of 1–2 [8]. In addition, to satisfy the target performance required, the rotor was designed to maximize the no-load air gap magnetic flux density.

The stator is initially designed using a mathematical method. The motor output characteristics were evaluated taking into account the magnetomotive force (MMF) of the armature, which influences the shape of the stator. Subsequently, armature MMF is determined based on the results of the evaluation. The armature MMF is related to the slot area through a proportional relationship

$$A_{\text{slot}} = \frac{2 \cdot m}{f_{\text{fill}} \cdot J \cdot n_{\text{slot}}} F_{\text{a}} \tag{1}$$

where A_{slot} is the slot area, F_{a} is the armature MMF, m is the number of phases, f_{fill} is the fill factor, J is the current density, and n_{slot} is the number of slots. Knowing the calculated slot area, the tooth width and the yoke thickness can be evaluated. Fig. 2 shows the structure of the initial model. To determine the number of turns of the armature, the line-to-line voltage and the current are evaluated. The number of turns of the armature is determined according to the power specifications. Fig. 3 shows that the saturation of

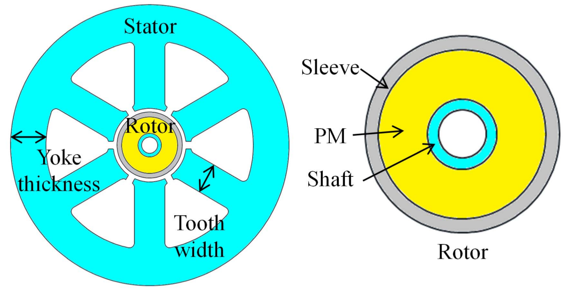

Fig. 2. Initial model structure of the UHS SPMSM.

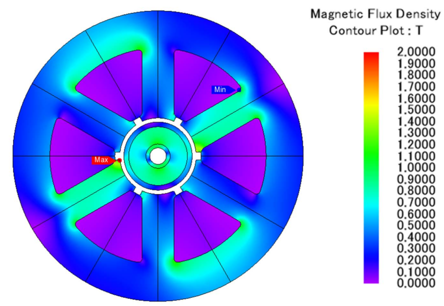

Fig. 3. Stator magnetic flux density distribution under load of the initial model.

the stator is low. Consequently, the output power density can be improved by reducing the outer diameter of the stator. The stator optimal design is obtained through the kriging surrogate model-based design process.

III. KRIGING SURROGATE MODEL

The surrogate model is a functional relationship between the design variable and the response, and it ensures a low computational cost, good accuracy, and very reliable performance. The kriging surrogate model is part of the surrogate models and is highly predictive for both linear and nonlinear responses [6], [10]. The kriging surrogate model is defined as follows:

$$\hat{Y}(x) = \boldsymbol{f}(x)^T \hat{\boldsymbol{\beta}} + \boldsymbol{r}(x)^T \boldsymbol{R}^{-1}\left(\boldsymbol{Y} - \boldsymbol{F}\hat{\boldsymbol{\beta}}\right) \tag{2}$$

where $\boldsymbol{f}(x)$ is the vector of known regression functions, $\hat{\boldsymbol{\beta}}$ is the vector of unknown regression coefficients, $\boldsymbol{r}(x)$ is the correlation vector between the design points and the prediction points, $\boldsymbol{R}$ is the correlation matrix between the design points, $\boldsymbol{Y}$ is the response matrix of the design points, and $\boldsymbol{F}$ is the vector of the regression function matrix [6], [10]. The correlation matrix is defined by a correlation function. The Gaussian correlation function is defined as

$$R = \exp\left(-\theta\left(s_i - s_j\right)^2\right) \tag{3}$$

where θ represents the correlation coefficient, while s_i and s_j are the vectors of the design points i and j, respectively [6].

IV. DESIGN OF THE KRIGING SURROGATE MODEL

A. Design Process

The design process based on the kriging surrogate model is shown in Fig. 4. To reduce the time required for the three-dimensional FEA (3D FEA) of the stator iron loss and

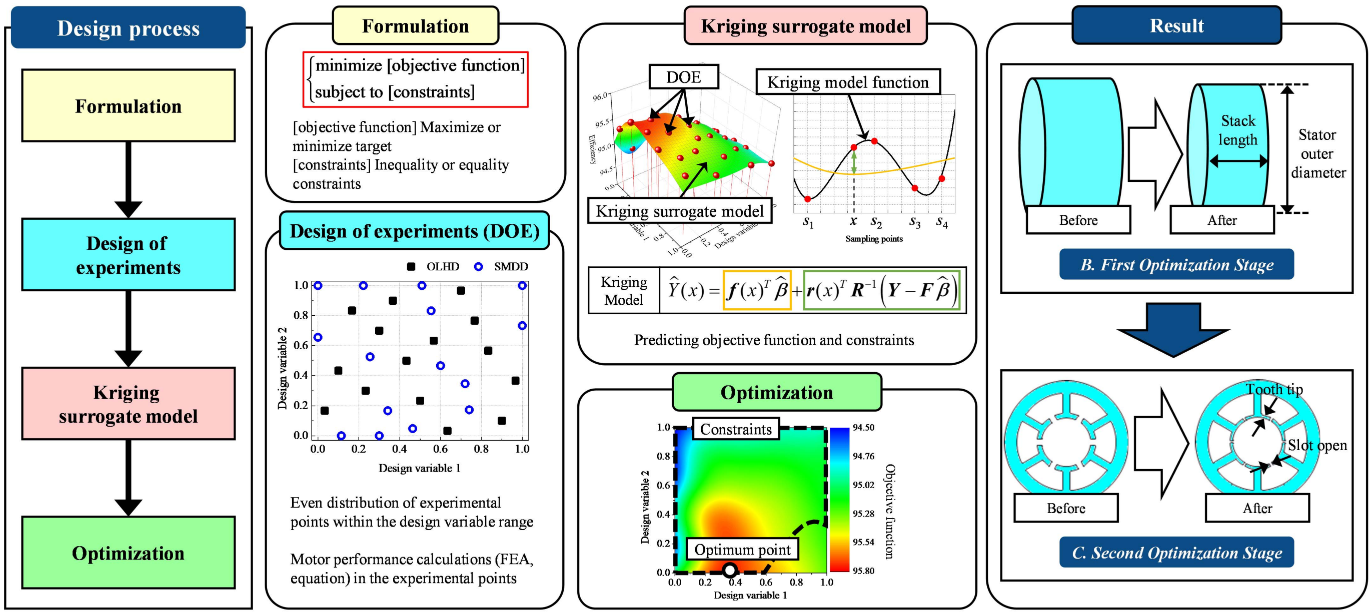

Fig. 4. Proposed kriging surrogate model-based design process.

rotor eddy current loss, the design process is divided into two stages: size determination and loss minimization. When dividing the motor parameters, the size determination step uses the parameters that do not require 3-D FEA, and the loss minimization step uses the parameters that require 3-D FEA. In fact, they require a different number of experimental points, a different objective function to define the design problems. For example, if the number of experimental points is n in the size determination step, the number of experimental points can be set to $n/20$ in the loss minimization step. The advantages of this method are as follows.

1) Simplify optimization problem definition.
2) Reduced computation time.
3) High prediction accuracy of motor performances versus analysis time.

In both the stages, some optimization techniques are applied. First, problem optimization minimizes the objective function while satisfying the constraints. Next, the design of experiments (DOE) is applied to the selected design variables, and a kriging surrogate model is defined. In the kriging model shown in Fig. 4, the terms indicated by the yellow square box are the estimators of the global model and are determined using the generalized least squares method. In the same figure, the term indicated by the green square box is the local model and represents the deviation from the estimated mean model [6], [9]. Finally, the kriging surrogate models are used to determine the model that best satisfies the objective function and the constraints. As a result, the chosen model, compared with the model obtained using the conventional design methodology, ensures 1.4% reduction in the stator outer diameter, 11.8% reduction in the stack length, and 6.4% reduction in the total losses.

B. First Optimization Stage: Size Determination

Since the stator saturation of the initial model is low, there is a possibility that the outer diameter of the stator may be reduced. In addition, the stack length should be reduced

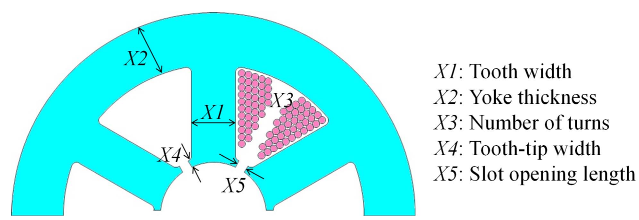

Fig. 5. Design variables.

to ensure space for the end coil and improve the output power density. An optimization technique is applied for size determination. The objective function is defined to minimize the stack length, and the constraints are set according to the electrical specifications. The objective function is the "target" that can be minimized or maximized, while the constraints can be defined as equality or inequality constraint.

The optimization problem is expressed as follows:

$$\begin{aligned} &\min\ L_{\mathrm{stk}} \\ &\text{s.t.}\ J \le J_{\max} \\ &\quad V_{\text{line-to-line}} \le V_{\text{line-to-line max}} \\ &\quad D_{\mathrm{s}} \le D_{\mathrm{s\,max}} \\ &\quad T = T_{\text{target}} \end{aligned} \tag{4}$$

where L_{stk} is the stack length, J is the current density, $J_{\max}$ is the maximum current density, $V_{\text{line-to-line}}$ is the line-to-line voltage, $V_{\text{line-to-linemax}}$ is the maximum line-to-line voltage, D_{s} is the stator outer diameter, D_{smax} is the maximum value of the stator outer diameter, T is the torque, and T_{target} is the target torque used to ensure output power at the maximum rotational speed.

As shown in Fig. 5, the tooth width ($X1$), the yoke thickness ($X2$), and the number of turns ($X3$) are the design variables. The DOE ensures that the experimental points are uniformly distributed within the range of the design variables. Subsequently, the responses are evaluated (using the FEA or the equations) according to the value of each design variable at

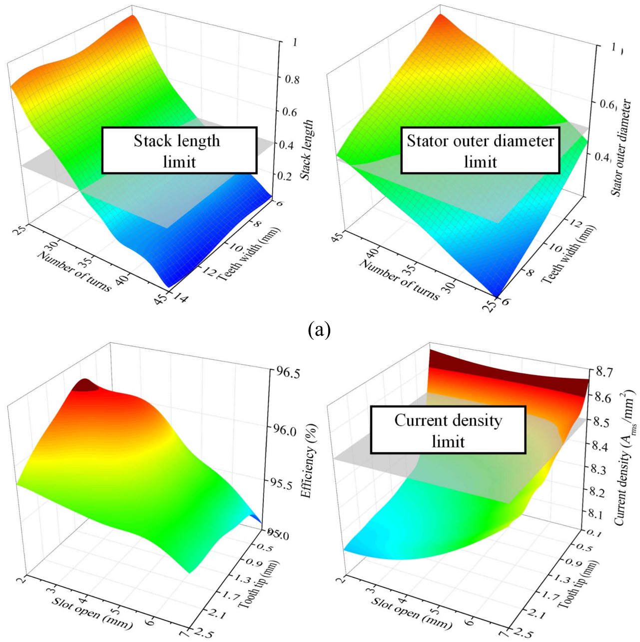

Fig. 6. Kriging surrogate models. (a) Stack length and stator outer diameter. (b) Efficiency and current density.

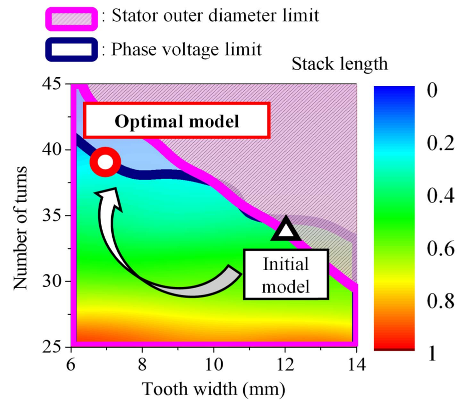

Fig. 7. Size optimization result.

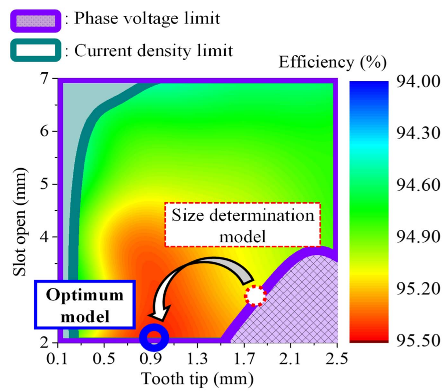

Fig. 8. Loss minimization result.

the experimental point. Responses refer to the values obtained at the experimental point, which are then used to generate the kriging surrogate model. The JMAG is used to evaluate the responses.

Finally, the kriging surrogate model is created, and the stator outer diameter, stack length, and line-to-line voltage are the responses to be predicted by the kriging surrogate model. If the motor is designed using a kriging surrogate model, the nonlinearity of the core according to the design variable can be taken into consideration. The armature MMF changes according to the number of turns, and if the current is constant, these variations affect the magnetic flux density of the stator core. Since the saturation of the core significantly influences the motor size, it is considered using the kriging surrogate model. Fig. 6(a) shows the kriging surrogate model used to determine the size of the motor. In addition, the optimal model, defined through the kriging surrogate models, which minimizes the stack length and satisfies the electrical specification, is shown in Fig. 7.

C. Second Optimization Stage: Loss Minimization

The iron loss, the rotor eddy current loss, the ac copper loss, and the windage loss are minimized by changing the stator shape. As mentioned earlier, the optimization technique is applied to minimize the motor losses. The constraints to minimize the motor losses are the electrical specifications and the target torque. The optimization problem is expressed as follows:

$$\begin{aligned} \min\ & P_{\text{loss}} (= \text{maximize } \eta) \\ \text{s.t.}\ & J \leq J_{\max} \\ & V_{\text{line-to-line}} \leq V_{\text{line-to-line max}} \\ & D_{\text{s}} \leq D_{\text{s max}} \\ & T = T_{\text{target}} \end{aligned} \tag{5}$$

where P_{loss} is the sum of the stator iron loss, rotor eddy current loss, ac copper loss, and windage loss, while η is the motor efficiency.

As shown in Fig. 5, the design variables are the tooth-tip width ($X4$) and slot opening length ($X5$). Moreover, in this case, the DOE is performed within the range of the design variables. Since the stator iron loss and the rotor eddy current loss are significant due to the high rotational speed, the UHS SPMSM is designed using the kriging surrogate model. Since the stator iron loss must consider the magnetic path in the z-axis direction, and the rotor eddy current loss must consider the path of the eddy current, they are evaluated through 3-D FEA. In addition, the high frequency of the UHS SPMSM input current causes a high ac copper loss, which is taken into consideration by the kriging surrogate model. The ac copper loss is evaluated by 2-D FEA.

The optimal model that minimizes the motor losses while satisfying the constraints is shown in Fig. 8, and it is obtained using the kriging surrogate model shown in Fig. 6(b). The kriging surrogate model was compared with the FEA to verify the accuracy of its predictions. The efficiency of the optimal model predicted through the kriging surrogate model is 95.5% and the efficiency calculated by the FEA result for the optimal model is 95.4%. Since the difference between the two efficiencies is not much, the validity of the design obtained using the kriging surrogate model can be confirmed. In addition, since the objective of the proposed design process of reducing the size and increasing the efficiency while meeting electrical

TABLE III
RESULTS OF COMPARING THE INITIAL MODEL AND OPTIMAL MODEL

Parameters	Initial model	Optimal model
Stator diameter / Stack length (mm)	115 / 74.6	113.4 / 65.8
Tooth width / Yoke thickness (mm)	12.5 / 14.7	7 / 15.9
Tooth-tip width (mm)	2	0.9
Slot opening length (mm)	3	2
Number of turns	34	39
Motor volume (mm^3)	774862	664572
Volume of PM (mm^3)	26136	23053

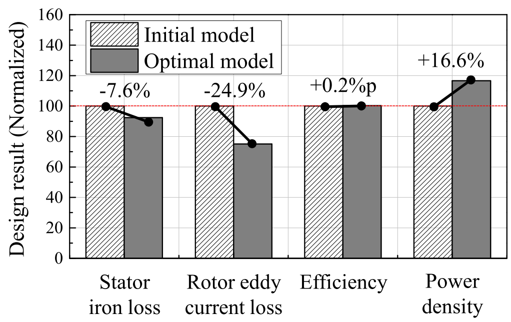

Fig. 9. Comparison of the initial model and the optimal model.

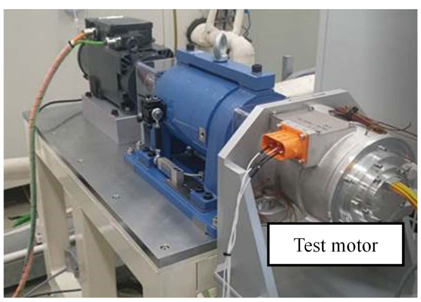

Fig. 10. Experimental setup for the no-load test of prototype.

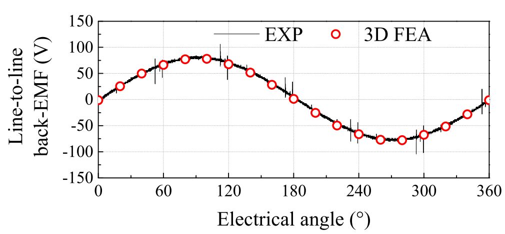

Fig. 11. Comparison of test and 3-D FEA no-load back EMF waveform.

specifications has been achieved, the validity of the proposed design process was confirmed.

V. Experimental Validation

Table III and Fig. 9 show the results of the comparison between the initial model and the optimal model. The optimal model designed using the kriging surrogate model reduces the motor volume, stator iron loss, and rotor eddy current loss by 14.2%, 7.6%, and 24.9%, respectively, more than the model designed using the conventional design methodology. Therefore, an optimal model that minimizes the motor size and losses while satisfying the power specification was obtained. In addition, the power density of the motor was improved by 16.6%, and the efficiency was increased by 0.2%. To verify the validity of the designed model, a prototype (see Fig. 10) was realized, and a no-load experiment was carried out at the rotational speed of 76 kr/min at 20 °C. Fig. 11 shows that the line-to-line back electromotive force (back EMF) evaluated with the no-load test is in good agreement (3.1% error) with the line-to-line back EMF evaluated with 3-D FEA. This test proved the validity of the designed model. As a load test of the motor, a centrifugal compressor system test was performed. Since it is practically difficult to prepare a torque sensor that can be used at a high rotational speed of 110 kr/min, the torque was indirectly estimated using the back EMF constant as described in [7]. The relative error between the test torque and the FEA torque was found to be less than 3.36%.

VI. Conclusion

In this article, the kriging surrogate model-based design of a UHS SPMSM was performed. The two-step optimal design process considering accuracy and computation time using the kriging surrogate model was presented. The designed UHS SPMSM through the proposed design process satisfies the electrical specifications while reducing the size and improving efficiency compared with the initial model. The design process proposed in this article can be applied to optimize the design of UHS SPMSM to which high-frequency current is applied with low computation time.

Acknowledgment

This work was supported by the Research and Development Program of Ministry of Trade, Industry and Energy/Korea Evaluation Institute of Industrial Technology under Grant 20010986.

References

[1] D.-M. Kim, J.-H. Kim, S.-G. Lee, M.-R. Park, G.-H. Lee, and M.-S. Lim, "Estimation method for rotor eddy current loss in ultrahigh-speed surface-mounted permanent magnet synchronous motor," *IEEE Trans. Magn.*, vol. 57, no. 2, pp. 1–5, Feb. 2021.

[2] Z. Zhang, Z. Deng, Q. Sun, C. Peng, Y. Gu, and G. Pang, "Analytical modeling and experimental validation of rotor harmonic eddy-current loss in high-speed surface-mounted permanent magnet motors," *IEEE Trans. Magn.*, vol. 55, no. 2, pp. 1–11, Feb. 2019.

[3] F. Zhou, J. Shen, W. Fei, and R. Lin, "Study of retaining sleeve and conductive shield and their influence on rotor loss in high-speed PM BLDC motors," *IEEE Trans. Magn.*, vol. 42, no. 10, pp. 3398–3400, Oct. 2006.

[4] M.-S. Lim, S.-H. Chai, J.-S. Yang, and J.-P. Hong, "Design and verification of 150-krpm PMSM based on experiment results of prototype," *IEEE Trans. Ind. Electron.*, vol. 62, no. 12, pp. 7827–7836, Dec. 2015.

[5] M.-S. Lim, J.-M. Kim, Y.-S. Hwang, and J.-P. Hong, "Design of an ultra-high-speed permanent-magnet motor for an electric turbocharger considering speed response characteristics," *IEEE/ASME Trans. Mechatronics*, vol. 22, no. 2, pp. 774–784, Apr. 2017.

[6] S. Kim, S.-G. Lee, J.-M. Kim, T. H. Lee, and M.-S. Lim, "Robust design optimization of surface-mounted permanent magnet synchronous motor using uncertainty characterization by bootstrap method," *IEEE Trans. Energy Convers.*, vol. 35, no. 4, pp. 2056–2065, Dec. 2020.

[7] J.-H. Kim, D.-M. Kim, Y.-H. Jung, and M.-S. Lim, "Design of ultra-high-speed motor for FCEV air compressor considering mechanical properties of rotor materials," *IEEE Trans. Energy Convers.*, early access, Mar. 1, 2021, doi: 10.1109/TEC.2021.3062646.

[8] R. G. Budynas, *Shigleys Mechanical Engineering Design*. New York, NY, USA: McGraw-Hill, 2011.

[9] S.-G. Lee, S. Kim, J.-C. Park, M.-R. Park, T. H. Lee, and M.-S. Lim, "Robust design optimization of SPMSM for robotic actuator considering assembly imperfection of segmented stator core," *IEEE Trans. Energy Convers.*, vol. 35, no. 4, pp. 2076–2085, Dec. 2020.

[10] L. Lebensztajn, C. A. RondiniMarretto, M. Caldoracosta, and J.-L. Coulomb, "Kriging: A useful tool for electromagnetic device optimization," *IEEE Trans. Magn.*, vol. 40, no. 2, pp. 1196–1199, Mar. 2004.